J Wood Sci (2004) 50:209–216
DOI 10.1007/s10086-003-0559-1

ORIGINAL ARTICLE

Wook Kang · Nam-Ho Lee

Relationship between radial variations in shrinkage and drying defects of tree disks

Received: September 25, 2002 / Accepted: May 21, 2003

Abstract This study was conducted to investigate the relationship between radial variations in shrinkage and drying behavior of larch disks during radio-frequency/vacuum (RF/V) drying. Despite considerable variations in shrinkage both within and between logs, some trends were observable for each log. Actual radial shrinkage was much larger than free radial shrinkage with a ratio of tangential shrinkage (α_T) to radial shrinkage (α_R) ranging from 1.27 to 1.62. If the α_T/α_R ratio of larch was about 2.5, the relative displacement was theoretically estimated to be 1.6 to 1.65, showing good agreement with the experimental results. The results showed that the formation of V-cracking was closely related to the actual differential shrinkage, which is the difference between the estimated tangential shrinkage and actual radial shrinkage after drying.

Key words Larch disk · Differential shrinkage · V-crack · Drying

Introduction

Effective utilization of small-diameter logs from the thinning of plantation trees has been an important issue in recent years.[1] The tree disk, which is cross cut from a log, for making wood artifacts is one way to effectively utilize wood, because of the potential for achieving high yields during the sawing process and aesthetic values. However, disk drying is much more difficult than drying lumber because of severe checking problems. Checks during the disk drying are caused by differences in shrinkage. One type is due to the moisture gradient across the disk thickness, and the other is due to the transverse anisotropy of wood and the difference in drying rates and shrinkages between sapwood and heartwood. They can be termed longitudinal and transverse differential shrinkage, respectively. In this study, however, we are only concerned with the transverse one because the moisture gradient across the disk thickness can be neglected in radio-frequency vacuum (RF/V) drying.

Wood varies widely with species and there are also variations within a species as well as within an individual tree. Such variations make it difficult to predict the performance of wood.[2] One of the main differences between sawn lumber and tree disks is that tree disks always include juvenile wood. The juvenile wood exhibits certain inherent trends in wood properties from pith to bark. In general, most of tree disks have pith displaced from their center, which gives some degrees of eccentricity. Such eccentricity renders tree disks highly inhomogeneous, making it difficult to predict drying behavior.

Thus, it is difficult to reduce the differential shrinkage of a tree disk caused by anisotropy regardless of the drying methods used. In theory, the drying stress due to the radial differential shrinkage may be approximated if the information on tangential and radial shrinkage, mechano-sorptive (MS) constants, and variation from pith to bark is available.[3] However, much less attention has been paid to understanding radial variations in the physico-mechanical properties of trees, particularly for rapidly grown plantation trees, primarily because tree disks or logs from such trees have rarely been utilized. Furthermore, much of the existing information available from published work has come from normal wood, where the focus has been on radial variation between trees and not within a tree.[4,5]

In general, young trees have large juvenile and abnormal zones. There are few studies on the degree of the deviation from axisymmetry of tree disks with growth eccentricity. Understanding the trends of physico-mechanical properties of a tree disk from pith to bark, as well as along the annual ring (i.e., periphery), is very important for mathematical simulation of drying behavior.

This study was undertaken to investigate effects of some basic parameters on the drying behavior of tree disks. These parameters include the radial variation of specific gravity

W. Kang (✉) · N.-H. Lee
Department of Forest Products, College of Agriculture, Chonbuk National University, Chonju, Chonbuk 561-756, Republic of Korea
Tel. +82-63-270-2623; Fax +82-63-270-2631
e-mail: kawook53@cricmail.net

Table 1. Basic parameters of the tree log bottom and top

Measured parameters	Log number				
	1	2	3	4	5
Diameter (cm)					
D_{ns}	34.4 (28.5)	28.4 (25.8)	28.9 (26.0)	30.4 (25.9)	31.0 (27.1)
D_p	34.0 (27.9)	27.0 (25.0)	29.4 (25.7)	31.6 (24.0)	35.1 (27.8)
Length (cm)	180	180	180	270	270
Heartwood (%)	58.1 (50.7)	50.5 (47.0)	63.5 (59.4)	55.3 (50.7)	59.1 (54.4)
Growth eccentricity (%)	34 (15)	14 (12)	11 (7)	9 (4)	13 (12)
No. of annual rings	28 (25)	23 (22)	27 (25)	21 (17)	33 (32)
No. of disks for drying	36	32	34	44	59

Numbers in parentheses are the values for the log top
D_{ns}, diameter in the direction along the north and south radii; D_p, diameter perpendicular to the direction along the north and south radii

Table 2. The average deviation from axisymmetry of disks (%)

	Log number					Total
	1	2	3	4	5	
Sample size	32	28	29	40	82	211
Roundness	1.41 ± 1.07	3.00 ± 1.47	0.75 ± 0.62	3.97 ± 1.80	5.16 ± 3.80	3.90 ± 3.09
Growth eccentricity	23.5 ± 5.2	14.0 ± 1.6	8.6 ± 2.3	7.4 ± 4.2	17.0 ± 7.7	15.6 ± 7.9

(SG), shrinkage along the radial and longitudinal directions, and the relationship between shrinkage and formation of checking during RF/V drying of larch (*Lalix kaempferi*).

Materials and methods

Basic properties of logs

Five larch logs with an approximate diameter of 30 cm were purchased from a local market. Three logs were 180 cm long and two were 270 cm long. The shapes of log bottom and top including the percentage of heartwood were calculated using an image analysis package (Olympus BMI plus v2.19, Korea). The results summarized in Table 1 show that the percentage of heartwood increased with an increase in the number of annual rings in the disks.

The growth eccentricity (GE) represents the deviation of pith from the geometrical center and was defined as

$$GE = \frac{r_s - r_n}{D_{ns}} \times 100 \qquad (1)$$

where r_s and r_n represent the south and north radius of the log as shown in Fig. 1a. D_{ns} is the diameter of the log that is the sum of the south and north radii. The eccentricity of tree disks was greater for disks from the tree bottom than those from the tree top. The roundness deviation (RD) of logs was defined by Eq. 2.

$$RD = \frac{\left|D_{ns} - D_p\right|}{D_{ns}} \times 100 \qquad (2)$$

where D_p represents a diameter perpendicular to D_{ns}. It was the least for Log 3 and the greatest for Log 5. Tree disks of

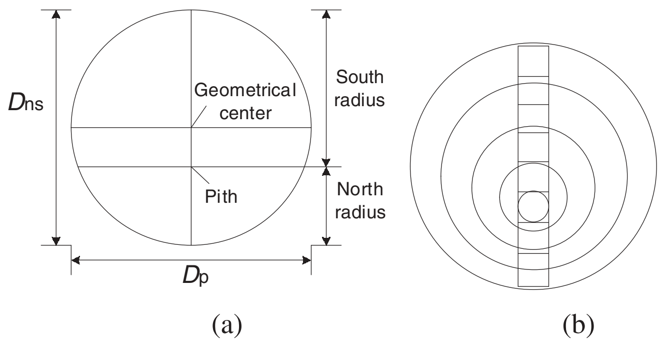

Fig. 1a,b. Specimens for measuring physical properties. **a** The definition of disk shape. **b** The preparation of specimen for measurement of specific gravity and free shrinkage. D_{ns}, diameter in the direction along the north and south radii; D_p, diameter perpendicular to the direction along the north and south radii

3-cm thickness along the longitudinal direction were successively cut from the logs for the following experiments. In turn, Log 1 showed the greatest eccentricity and Log 4 showed the least (Table 2).

Three disks were selected from the bottom, middle, and top of each log as shown in Fig. 1b. Each disk was divided along the north and south direction, which were used for measuring SG and free shrinkage from pith to bark. Note that free shrinkage is the unrestrained shrinkage without internal stresses while shrinkage of tree disks have inevitably been restrained due to anisotropy. Dimensions of the cross section samples were 5 × 5 × 3 cm (R × T × L). Three samples (5 mm thick) were obtained from one cross section, and marked to identify their original position. Volumetric shrinkage was estimated from the summation of radial and tangential shrinkages. All measurements were made up to

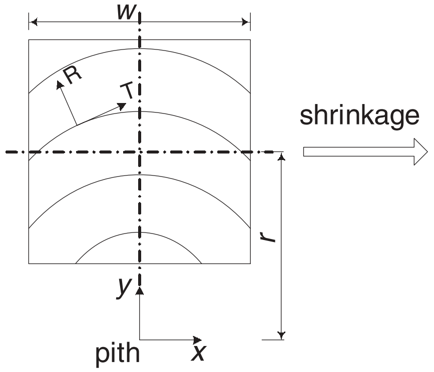

Fig. 2. The change of the apparent tangential shrinkage in the middle of the specimen depending on the distance from the pith. *R*, radial direction, *T*, tangential direction, *w*, width of specimen, *r*, distance from pith to the middle of specimen

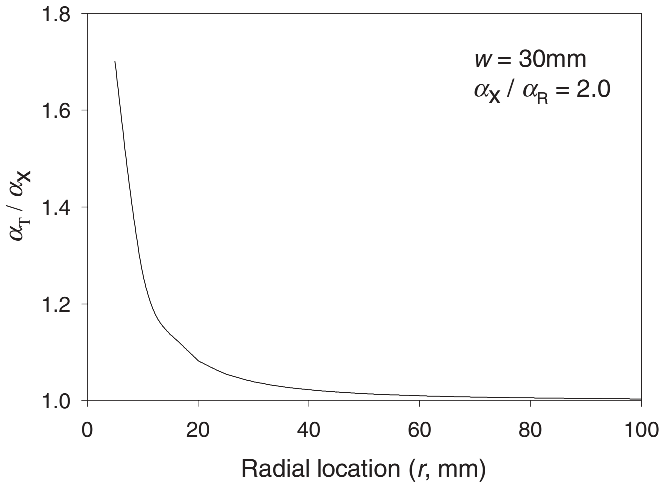

Fig. 3. The ratio of apparent shrinkage (α_T) to actual shrinkage (α_x) versus radial location

0.01 mm with a dial gauge. The SG was obtained from oven-dry weight and the green volume of a specimen. Two pairs of lines perpendicular to each other were drawn on the disk to determine shrinkage of disks after drying. One line was first drawn along the north and south direction and then the other one was drawn in the perpendicular direction. Changes in the lengths of these lines were measured using an image analyzer.

Tangential shrinkage

The radius of curvature depends on the distance from the pith. Although the actual tangential shrinkage (α_T) is constant outward from the pith, the apparent tangential shrinkage (α_x) obtained from the specimens varies with the radius of curvature. It results in cupping due to the differential shrinkage although there are no differences in moisture content (MC) gradient and shrinkage between the bottom and top within a specimen (Fig. 2).

By considering the effects of ring curvature, the relationship between α_x and α_T can be derived as[6,7]

$$\alpha_T = \frac{\alpha_x w - \alpha_R\left(w - 2r\tan^{-1}\dfrac{w}{2r}\right)}{2r\tan^{-1}\dfrac{w}{2r}} = \alpha_R + \frac{(\alpha_x - \alpha_R)w}{2r\tan^{-1}\dfrac{w}{2r}} \quad (3)$$

where α_R represents radial shrinkage and w is width of specimen.

Using the Eq. 3, the effect of the radius of curvature on the apparent shrinkage should be taken into account in measuring the actual tangential shrinkage in the radial direction because large errors may occur near the pith. In the case of $\alpha_x/\alpha_R = 2.0$ and $\omega = 20$ mm, considerable errors resulted at the location below 20 mm from the pith without taking the radius of curvature into consideration as shown in Fig. 3.

Radio-frequency/vacuum

The RF/V drying of the samples was carried out in a laboratory kiln.[8] The output of the RF generator was 7 kW at a fixed frequency of about 13 Mhz. The ambient pressure during the RF/V drying test was lowered to an absolute value of around 50 mmHg. Wood temperature during drying began at 42°C and was gradually increased by 3°–6°C per day, to a maximum of 54°C at the end. After RF/V drying, drying defects were visually evaluated and the actual shrinkage of disks along the north and south radii was measured.

Results and discussion

Radial variation of specific gravity

Figure 4 shows the variation in specific gravity along the radial direction. The relative radial location is presented as a fraction of the pith to bark distance with the largest value of 1. Also, the SG in the north and south radii is represented with minus and plus signs, respectively.

It has been reported that the trend of SG variations may be of two different types along the radial direction for larch.[9] In Type 1, SG increases from pith to bark. In Type 2, SG is high near the pith with a decrease outward for the first few growth rings, and then an increase to a maximum at the bark. However, the SG variation in this study did not follow either of these two types. It initially increased from the pith to outer half distance and then decreased toward the bark. The SG of Logs 1, 3, and 5 that had larger growth eccentricity than Logs 2 and 4 decreased from the pith, and did not show any significant relationship with the location along the height. The results of this study are consistent with those of Kollmann and Cote[10] and Kim.[11] Kim[11] reported that the width of annual rings of 38-year-old larch showed that the ring density decreased from the pith to the 16th ring and increased continuously until the 38th ring. This result indicates a close relation to the SG variation pattern of this study.

As shown in Table 3, the SG of sapwood is lower than that of heartwood except for Log 2, and the SG near the

Table 3. Specific gravity of heartwood and sapwood of Korean larch

Log number	Sapwood	Heartwood	Mixed	Pith
1	0.40 ± 0.03 (18)	0.44 ± 0.03 (57)	0.43 ± 0.03 (75)	0.43 ± 0.05 (9)
2	0.43 ± 0.01 (18)	0.40 ± 0.03 (52)	0.41 ± 0.03 (70)	0.35 ± 0.02 (3)
3	0.42 ± 0.01 (18)	0.43 ± 0.02 (52)	0.42 ± 0.02 (70)	0.36 (1)
4	0.40 ± 0.01 (17)	0.42 ± 0.03 (49)	0.41 ± 0.03 (66)	0.38 ± 0.01 (9)
5	0.43 ± 0.04 (18)	0.45 ± 0.03 (60)	0.44 ± 0.03 (78)	0.44 ± 0.04 (6)
Average	0.41 ± 0.02 (89)	0.42 ± 0.03 (270)	0.42 ± 0.03 (359)	0.40 ± 0.04 (28)

Numbers in parentheses represent the numbers of specimens

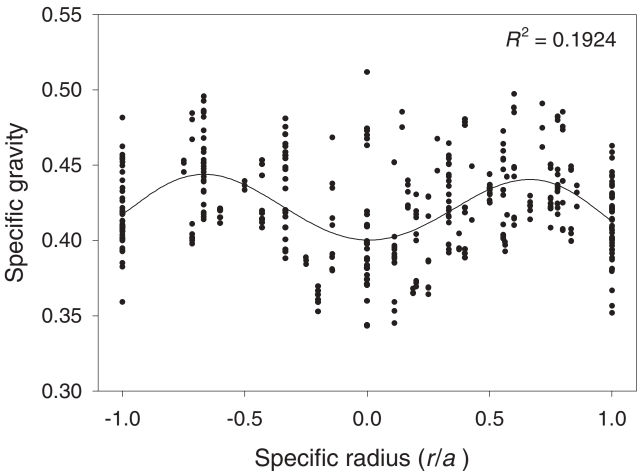

Fig. 4. Variation of specific gravity in the radial direction. Negative specific radius correlates to the north radius; positive specific radius correlates to the south radius. *a*, radius of disk; *r*, distance from pith

pith is lower than that of the other log areas except for Logs 1 and 4. The overall averages of SG in the north and south radii are 0.426 ± 0.031 and 0.425 ± 0.029, respectively, with no statistically significant difference.

Radial and tangential shrinkage in radial direction

The radial and tangential shrinkage along the radial direction is given in Fig. 5. The overall shrinkage values generally increased from pith to bark, which is consistent with the previous report of Kim[11] who showed the dependence of the shrinkage on microfibril angle and partially on the formation of heartwood. The shrinkage changes of Logs 2 and 4 were typical patterns along the radial direction, but this was not the case for Logs 1, 3, and 5. In particular, the shrinkage of Logs 1 and 3 in the south radius decreased outward from the pith and increased toward the bark. The low tangenial shrinkage might be due to a compression wood zone that has large longitudinal shrinkage and small transverse shrinkage. For Log 5, the radial trend did not show a specific pattern.

Both the radial and tangential shrinkages of the sapwood along the north radius were greater than those of the heartwood along the south radius (Tables 4, 5). Because compression wood has exceptionally high longitudinal shrinkage and less volumetric shrinkage when compared with normal wood, the transverse shrinkage of compression wood is smaller than that of normal wood. The T/R ratio of compression wood is smaller than that of normal wood and it might be desirable to help prevent V-cracks during drying. The wood along the south radius seemed to contain compression wood, but there was no clear indication from the results. For most of the trees used, the α_T is two times greater than the α_R. For heartwood, there was a weak positive correlation between SG and volumetric shrinkage (R^2 = 0.139), while there was no significant correlation for sapwood (R^2 = 0.074). This result indicates that the variation of shrinkage along the radial direction is more likely to be related to the amount of heartwood extractives than the SG of wood. Mean shrinkage values could be used to predict average dimensional changes in batches of materials, but it cannot be applicable to individual disks because there is considerable variability within and between disks. All differential shrinkages of sapwood were greater than that of heartwood but the α_T/α_R ratio showed the opposite trend with the exception of Log 1. The position of maximum difference between tangential and radial shrinakge ($\alpha_T - \alpha_R$) varies in the logs. It should be noted that the nondimensional form of the α_T/α_R value is generally used, but radial deformation of tree disks has closer relation with $\alpha_T - \alpha_R$.[3]

Radial shrinkage and drying defects of tree disks

During the RF/V drying, uniform shrinkage of tree disks requires a proportional reduction of the diameter and of the circumference in order to maintain a circular cross section. The percentage of the decreases must be the same for both. Therefore, tangential stress is proportional to the differential shrinkage that is the difference between the reduction in circumference by tangential shrinkage and the reduction in diameter by radial shrinkage. V-cracks or heart checks occur when the tangential stress exceeds the maximum tensile strength. The occurrence of V-cracks has a close relationship with that of both sapwood and heartwood checks due to the stress superposition principle and stress concentration. Tensile strength perpendicular to grain is estimated to be 3800 $SG^{0.78}$(kPa) in green wood and 6000 $SG^{1.11}$(kPa) in wood with 12% MC with a coefficient of variation being 28%.[12] Therefore, the average might be assumed to be 1.9–2.4 MPa in the case of larch. The strength of 5% exclusion limit might amount to 1.0–1.3 MPa.

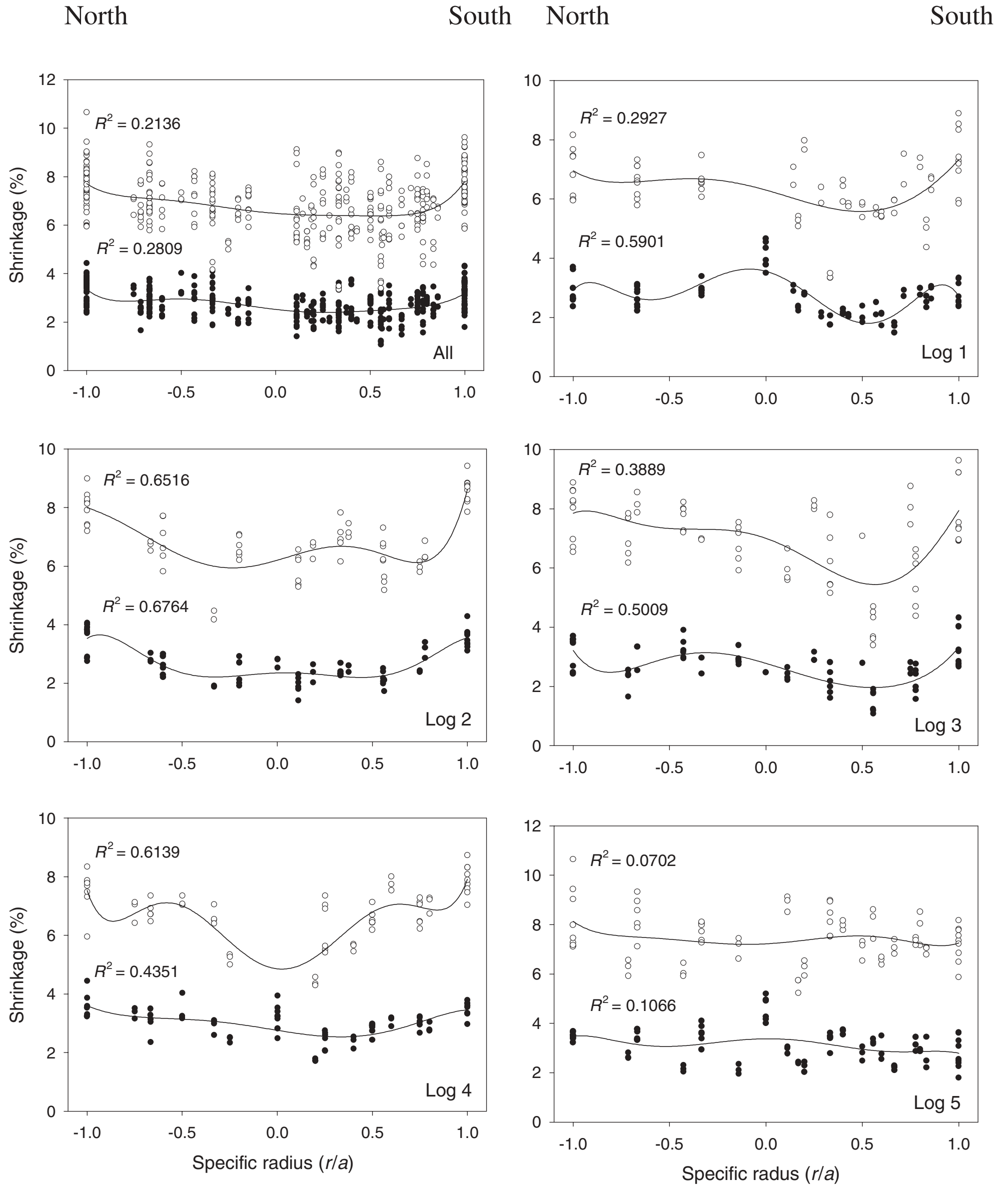

Fig. 5. Radial variation of the radial and tangential shrinkage for each log and combined results. *Open circles*, tangential shrinkage; *solid circles*, radial shrinkage

Kubler[13] assumed that the reduction in diameter was accomplished only by radial shrinkage because it was taken to be free of stress in the radial direction. However, Kang and Lee[3] reported that a considerable compressive stress occurs in the radial direction during drying. In addition, the Poisson's effect due to tensile stress in the tangential direction may further reduce the radial dimension more than that by free radial shrinkage, in which the reduction depends on ratios of elasticity and shrinkage of the tangential direction to those in the radial direction. Based on the model of Kang and Lee,[3] the relative displacement that is the ratio of actual radial shrinkage of disk to free radial shrinkage can be calculated due to the shrinkage and elasticity anisotropy as shown in Fig. 6. The actual shrinkage of the disk increases with the increase of shrinkage anisotropy and with the decrease of elasticity anisotropy.

In practice, uniform shrinkage might not occur and disks might reveal an ellipsoidal or irregular shape after drying.

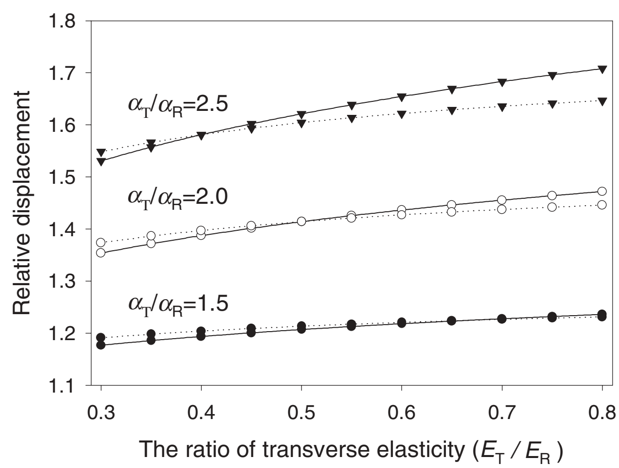

Fig. 6. The relative radial displacement by both elastic and mechanosorptive (MS) model[3] depending on the anisotropy. *Solid line*, elastic; *dotted line* MS model

Table 4. Free shrinkage of sapwood and heartwood from green to oven dry

Log number	n	Shrinkage (%)		$\alpha_T + \alpha_R$ (%)	$\alpha_T - \alpha_R$ (%)	α_T/α_R (%)
		α_T	α_R			
1						
Sapwood	17	7.18 ± 0.97	2.83 ± 0.44	10.00 ± 1.32	4.35 ± 0.74	2.56 ± 0.30
Heartwood	54	6.09 ± 1.00	2.47 ± 0.45	8.56 ± 1.34	3.61 ± 0.79	2.50 ± 0.43
Mixed	71	6.35 ± 1.09	2.56 ± 0.47	8.90 ± 1.46	3.79 ± 0.83	2.52 ± 0.40
Pith	7	–	4.08 ± 0.44	–	–	–
2						
Sapwood	18	8.30 ± 0.60	3.54 ± 0.44	11.84 ± 0.96	4.77 ± 0.41	2.37 ± 0.21
Heartwood	48	6.42 ± 0.77	2.38 ± 0.41	8.80 ± 1.01	4.04 ± 0.72	2.75 ± 0.49
Mixed	66	6.93 ± 1.12	2.72 ± 0.68	9.65 ± 1.70	4.22 ± 0.73	2.63 ± 0.47
Pith	3	–	2.72 ± 0.17	–	–	–
3						
Sapwood	18	7.89 ± 0.98	3.27 ± 0.57	11.16 ± 1.52	4.62 ± 0.52	2.44 ± 0.21
Heartwood	52	6.60 ± 1.39	2.50 ± 0.61	9.10 ± 1.92	4.10 ± 0.97	2.69 ± 0.39
Mixed	70	6.93 ± 1.41	2.70 ± 0.69	9.63 ± 2.03	4.23 ± 0.90	2.63 ± 0.37
Pith	1	–	2.45	–	–	–
4						
Sapwood	17	7.73 ± 0.62	3.53 ± 0.33	11.26 ± 0.55	4.20 ± 0.82	2.21 ± 0.28
Heartwood	48	6.48 ± 0.88	2.81 ± 0.48	9.28 ± 1.29	3.67 ± 0.58	2.33 ± 0.24
Mixed	65	6.80 ± 0.99	3.00 ± 0.55	9.80 ± 1.44	3.81 ± 0.69	2.30 ± 0.25
Pith	9	–	3.18 ± 0.43	–	–	–
5						
Sapwood	18	7.69 ± 1.10	3.14 ± 0.57	10.83 ± 1.40	4.55 ± 1.07	2.53 ± 0.58
Heartwood	60	7.39 ± 0.98	2.96 ± 0.57	10.35 ± 1.40	4.43 ± 0.77	2.55 ± 0.41
Mixed	78	7.46 ± 1.01	3.00 ± 0.57	10.46 ± 1.41	4.46 ± 0.84	2.55 ± 0.45
Pith	6	–	4.59 ± 0.49	–	–	–
Sub-total						
Sapwood	88	7.76 ± 0.94	3.26 ± 0.54	11.03 ± 1.33	4.50 ± 0.76	2.42 ± 0.36
Heartwood	262	6.62 ± 1.12	2.63 ± 0.56	9.25 ± 1.56	3.98 ± 0.83	2.57 ± 0.42
Mixed	350	6.91 ± 1.18	2.79 ± 0.62	9.70 ± 1.67	4.11 ± 0.84	2.53 ± 0.41
Pith	26	–	3.67 ± 0.81	–	–	–
Total	376	6.91 ± 1.18	2.85 ± 0.67	9.70 ± 1.69	4.11 ± 0.84	2.53 ± 0.41

α_T, tangential shrinkage; α_R, radial shrinkage

Table 5. Free shrinkage in the north and south radii from green to oven dry

	Log number					Total
	1	2	3	4	5	
North						
n	24	25	32	26	30	137
α_T (%)	6.72 ± 0.63	6.99 ± 1.11	7.48 ± 0.79	6.87 ± 0.82	7.61 ± 1.12	7.17 ± 0.97
α_R (%)	2.84 ± 0.37	2.85 ± 0.68	2.97 ± 0.52	3.22 ± 0.50	3.17 ± 0.62	3.01 ± 0.56
$\alpha_T - \alpha_R$ (%)	3.88 ± 0.53	4.15 ± 0.65	4.51 ± 0.66	3.65 ± 0.70	4.44 ± 0.90	4.16 ± 0.77
South						
n	47	41	38	39	48	212
α_T (%)	6.16 ± 1.22	6.89 ± 1.14	6.42 ± 1.64	6.76 ± 1.09	7.37 ± 0.94	6.74 ± 1.28
α_R (%)	2.41 ± 0.46	2.64 ± 0.67	2.45 ± 0.74	2.85 ± 0.54	2.90 ± 0.52	2.65 ± 0.61
$\alpha_T - \alpha_R$ (%)	3.75 ± 0.95	4.26 ± 0.78	3.97 ± 1.01	3.91 ± 0.67	4.47 ± 0.81	4.09 ± 0.89

However, it should be noted that the frequency of V-cracks decreases as the relative displacement increases, which is due to the decrease of the differential shrinkage.

Table 6 shows the actual radial shrinkage of tree disks after drying at which it was corrected to an MC of 8%. The actual radial shrinkage of disks was much larger than the free radial shrinkage, whose ratios, the relative displacements, ranged from 1.27 to 1.62 with the exception of Log 3 that had extremely low radial shrinkage in the south radius. The relative displacement is estimated to be 1.6–1.65 if the α_T/α_R ratio of larch is about 2.5 (Fig. 6). Therefore, it is in an agreement with the experimental results.

Table 7 shows a summary of data for checks and V-cracks after RF/V drying. Heartwood checks were severe in Logs 1 and 5. Sapwood checks occurred slightly with the exception of Log 1. V-cracks were severe in Logs 1, 3, and 5 that showed large differential shrinkage (Table 8). Thus, the growth eccentricity and roundness of tree disks was not related to V-cracks, but was closely related to the actual differential shrinkage (i.e., the difference between free tangential and actual radial shrinkage). In addition, as the number of annual rings increased, the percentage of heartwood increased. The frequency of V-cracks rose as the number of annual rings and the percentage of heartwood increased.

Table 6. Actual shrinkage of tree disks after drying

Log number	n	S_{ns}				S_p (%)
		North radius (%)	South radius (%)	Average (%)	Ratio[a]	
1	19	3.28 ± 1.90 (2.08 ± 0.27)	2.02 ± 2.23 (1.77 ± 0.34)	2.52 ± 1.57 (1.97 ± 0.47)	1.28	2.41 ± 1.57
2	17	3.53 ± 1.46 (2.09 ± 0.50)	3.08 ± 1.60 (1.93 ± 0.49)	3.20 ± 0.79 (1.98 ± 0.48)	1.62	3.27 ± 0.78
3	14	3.55 ± 1.19 (2.17 ± 0.38)	0.07 ± 1.66 (1.80 ± 0.54)	1.71 ± 1.07 (1.83 ± 0.45)	0.93	1.82 ± 1.07
4	25	2.57 ± 1.90 (2.27 ± 0.58)	3.98 ± 1.47 (2.09 ± 0.39)	3.35 ± 1.02 (2.20 ± 0.40)	1.52	3.23 ± 1.00
5	39	3.67 ± 1.43 (2.32 ± 0.45)	2.26 ± 1.70 (2.12 ± 0.38)	2.79 ± 1.2 (2.20 ± 0.42)	1.27	3.36 ± 1.2
Total	114	3.33 ± 1.64 (1.93 ± 0.47)	2.43 ± 2.07 (2.21 ± 0.41)	2.80 ± 1.25 (2.05 ± 0.45)	1.37	2.97 ± 1.28

Values in parentheses represent the free radial shrinkage from green to 8% moisture content
S_{ns}, shrinkage in the direction along north and south radii; S_p, shrinkage perpendicular to the direction along north and south radii
[a] Ratio represents the ratio of the actual to free radial shrinkage

Table 7. Drying defects of tree disks after radio-frequency/vacuum drying

Log number	n	V-crack			Heartwood (sapwood) checks	
		Defective disks (%)	Length of cracks (cm)	Width of cracks (cm)	Defective disks (%)	Length of checks (cm)
Total	163	18.4 (3.1)[a]	10.3	0.9	8.6 (4.9)[a]	4.9 (3.2)
1	31	12.9 (0.0)	11.5	0.8	16.1 (0.0)	4.6 (0.0)
2	25	12.0 (12.0)	6.2	0.4	4.0 (4.0)	2.7 (2.3)
3	24	37.5 (0.0)	11.2	0.9	0.0 (4.2)	0.0 (3.1)
4	27	3.7 (0.0)	2.9	0.1	0.0 (7.4)	0.0 (1.4)
5	56	23.2 (3.6)	10.8	1.0	14.3 (7.1)	5.4 (4.3)

[a] V-cracks or checks occurred with the lapse of 10 days after drying

Table 8. Actual shrinkage along the north and south radii from green to 8% moisture content

	Log number					Total
	1	2	3	4	5	
α_T[a] (%)	4.65 ± 0.80	5.09 ± 0.82	5.08 ± 1.03	4.93 ± 0.76	5.47 ± 0.74	5.07 ± 0.87
α_R[b] (%)	2.46 ± 1.54	3.24 ± 0.73	1.76 ± 1.04	3.29 ± 0.92	3.29 ± 0.92	2.88 ± 1.22
$\alpha_T - \alpha_R$ (%)	2.19	1.85	3.32	1.64	2.18	2.19

[a] Free tangential shrinkage based on oven dry method
[b] Actual shrinkage of disk after drying

Conclusion

Although there was a considerable amount of variation in shrinkage both within and between trees, it was possible to detect certain trends for each tree. This study suggested a correction method for the tangential shrinkage of rectangular specimens. Actual radial shrinkage of disks was much larger than free radial shrinkage, the ratios of which ranged from 1.27 to 1.62. If the α_T/α_R ratio of larch is about 2.5, the relative displacement was theoretically estimated to be 1.6–1.65, which shows good agreement with the experimental results. V-cracks were closely related to the actual differential shrinkage, which is the difference between the estimated tangential shrinkage and actual radial shrinkage after drying. Further study might be needed on the degree of axisymmetry in geometry including growth eccentricity, the deviation extent from a circular shape, and physico-mechanical properties. Also, it is necessary to investigate significant differences of shrinkage within and between trees.

Acknowlegments This work was supported by a grant from the Post-Doctoral Program, Chonbuk National University, Korea (2001). The authors thank Dr. A. Singh, Chonnam University, Korea, and Prof. S. Pang, University of Canterbury, New Zealand, for their valuable advice.

References

1. Kärki T (2001) Variation of wood density and shrinkage in European aspen (*Populus tremula*). Holz Roh Werkst 59:79–84
2. Zobel BJ, van Buijtenen JP (1989) Wood variation: its causes and control. Spinger, Berlin Heidelberg New York, p 1
3. Kang W, Lee NH (2002) Mathematical models to predict drying deformation and stress due to the differential shrinkage within a tree disk with radial variations. Wood Sci Technol 36:463–476
4. Shupe TD, Choong ET, Gibson MD (1995) Differences in moisture content and shrinkage between outerwood, middlewood, and corewood of two yellow poplar trees. Forest Prod J 45:85–90
5. Shupe TD, Choong ET, Gibson MD (1995) Differences in moisture content and shrinkage between innerwood and outerwood, of a single cottonwood tree. Forest Prod J 45:89–92
6. Kang W, Lee NH, Choi JH, Li C (2001) Variations of free shrinkage in larch log cross section and drying shrinkage during radio-frequency/vacuum drying. In: 2001 Proceedings of the Korean Society of Wood Science and Technology Fall Meeting. October 19–20 2001, Korea
7. Wiedenbeck JK, Hofmann K, Peralta P, Skaar C, Koch P (1990) Air permeability, shrinkage, and moisture sorption of lodgepole pine stemwood. Wood Fiber Sci 22:229–245
8. Kang W, Lee NH, Choi JH (2001) A radial distribution of moistures and tangential strains within a larch log cross section during radio-frequency/vacuum drying. Holz Roh Werkst (in press)
9. Panshin AJ, de Zeeuw C (1970) Textbook of wood technology, 3rd edn, vol 1. McGraw-Hill, New York, pp 252–253
10. Kollmann FP, Cote WA (1968) Principles of wood science and technology I. Solid wood. Springer, Berlin Heidelberg New York, pp 170–171, pp 178–179
11. Kim YC (1997) Variations in properties and qualities of major plantation-grown softwoods in Korea. PhD Dissertation. Kyung Hee University (in Korean)
12. Forest Products Laboratory (1999) Wood handbook. Gen. Tech. Rep. FPL-GTR-113. Madison, WI:U.S. Department of Agriculture, Forest Service, Forest ProductsLaboratory. pp 4–28
13. Kubler H (1975) Study on drying of tree cross sections. Wood Sci 7:173–181